



Design of Broadband Patch Antenna Using Modified Lumped Parameter

Yamini Pandey¹, Prof Pritesh Tiwari²
 PG Scholar(M.Tech)¹, ²Professor,
 Department of ECE^{1,2},
^{1,2}BIT, Bhopal(M.P), India

Yaminip297@gmail.com, priteshtiwari.15@gmail.com

Abstract— Patch antennas are among the smallest antennas used in communication. A meandering slot may change an MPA electrical length. This manuscript examines a modified rectangular Patch Antenna with a meandering slot utilizing HFSS. We present four meandering slot patch antennas. First, a single meandering slot impedance structure without slot lines. Second design is extended version of basic design with slot line. The third proposal is a dual meandered slot impedance structure. Fourth, a twin meandered structure with vertical and horizontal patch slots. The 4th design has the best 5.8 GHz return loss, bandwidth, antenna gain, and VSWR. -37dB, 850MHz, 1.02, 1.76dB respectively. The 4th design has larger bandwidth at higher simulation frequency than the 3rd, 2nd, and 1st designs (2 GHz to 6 GHz). At 5.3 GHz and higher, 4th design return loss is improved by 252.71%, 47.29%, and 66.96% as compression. Fourth-design antenna gain at 5.8 GHz is 58.55 percent higher than third-design. 4th design antenna gain is 2.15 dB more than 2nd and 3.74 dB greater than 1st. The 4th suggested design with twin meandering slots and modified vertical and horizontal slots is the best. Impedance improves sub-6 GHz patch antenna bandwidth, gain, return loss, and VSWR. The work opens the door for broadband antenna design with enhanced return loss and gain using microstrip patch slot impedance structure.

Keywords- FR4; lumped parameters; Meandered Slot; printed Impedance resonator; Broadband, Antenna Gain.

I. INTRODUCTION

Patch antenna consists of a metallic patch, generally copper, printed on a thin grounded dielectric substrate. A coaxial line or a coplanar microstrip line feeds the signal to the antenna. The metallic patch radiates and receives electromagnetic radiation. Shape, feeding method, and substrate arrangement vary.

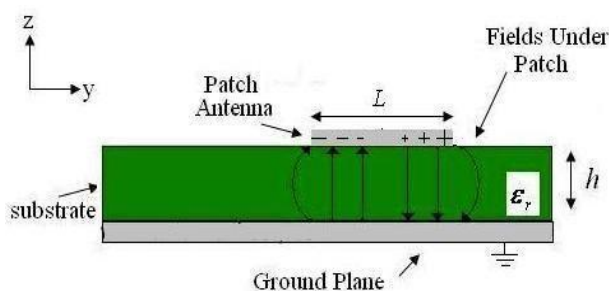


Fig. 1.1 The Basic of Microstrip Antenna

Figure 1.1 illustrates a MPA with double-sided PCB and a dielectric substrate. The fundamental model of an energized rectangular patch shows its electric field.

L =patch length, W =patch width, H =substrate height the electric field is zero at the patch's center, positive on one side, and negative on the other. Signal direction alters maximum and minimum fields. These fringe fields cause the patch to radiate. Dielectric constant about $2.2 \leq \epsilon_r \leq 12$. Changing the substrate material and thickness improves MPA performance, but increasing thickness introduces surface waves that decrease pattern and polarization. The substrate's dielectric constant ϵ_r should be low ($\epsilon_r < 2.5$) to enhance the fringing field [1]. While beginning the process of validating the design, it is critical to determine the fundamental parameters, fundamental features, and specifications of the provided antenna configuration. This should be done well in advance of the validation procedure. It is essential for us to ensure that the simulation process is carried out accurately and

without any mistakes, thus this is a very crucial consideration.

II. Design Procedure for Rectangular Patch Antenna

The design approach that will be employed [8,9] for the project's Procedure for designing a rectangular patch antenna will look like what is seen in figure 2.1.

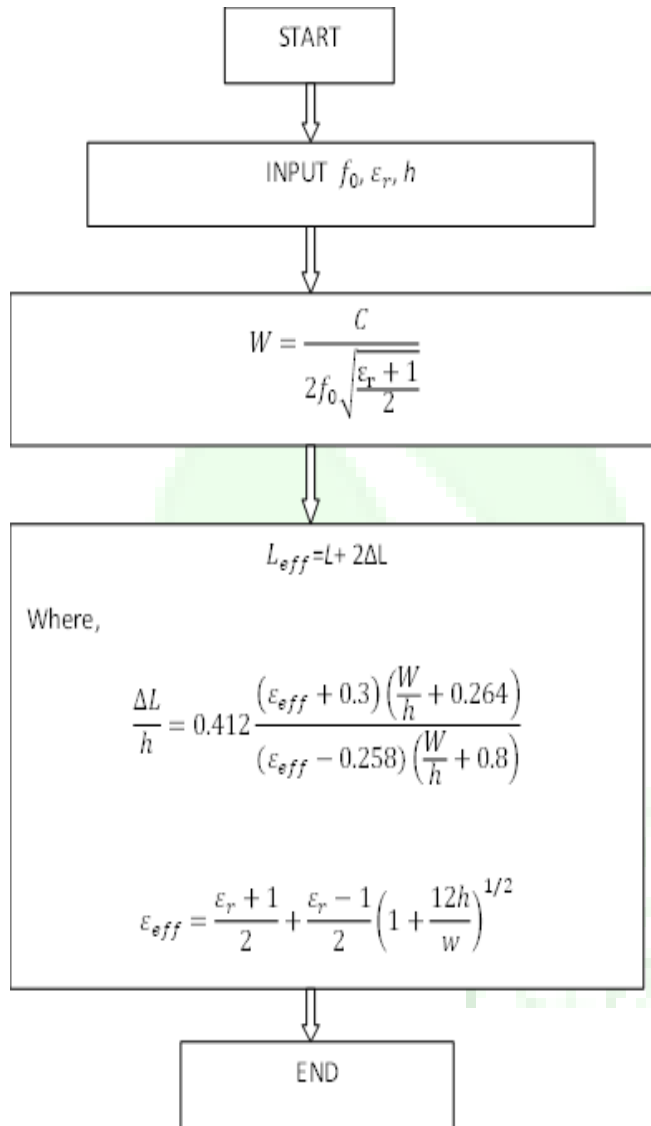


Fig. 2.1 Flow chart based on usual design procedure for rectangular patch antenna

Steps required for calculating width (W) and Length (L) of a conventional rectangular MPA

Step 1. Initially, select the desired resonant frequency, thickness and dielectric constant of the substrate.

Step 2. Obtain Width (W) of the patch by giving the value of ϵ_r And f_0 .

Step 3. Obtain Length (L) of the patch after determining ΔL and ϵ_r . It is also possible to determine the inset length of

the patch by taking the resonant frequency f_0 , width W and length L of the patch as input.

III. DESIGN OF PROPOSED WORK

The recommended antenna designs are modelled using analysis HFSS for a 2 GHz to 6 GHz sweep frequency to determine their performance. Different rectangular patch antenna impedance designs are shown and assessed (RPA).

Different antenna designs are integrated with meandering slot impedance structure-based patches, and the adjustment in vertical and horizontal slot structure together with meandered slot improves the traditional MPA's broadband capabilities, gain, and return loss. The four-patch antenna designs in this work have identical substrate designs and materials, but the top metallic patches are different.

(a) 1st Design of Single MSPA Model

First design is a single meandered slot impedance resonator. The suggested antenna is 32 mm 26 mm with a 1.6 mm thickness. The feed line and excitation point are both 6 mm. 1 mm wide and 5 mm long, the single meandered slot impedance resonator. The patch is 23 mm 15 mm and 5 mm from the origin in x- and y-axes. This portion has one meandering observation spot. Figure 1.6 shows the suggested antenna's dimensions. The highlighted region is our patch, and the red hue represents the x-z feed point. Each meandering slot has a 1 mm gap for consistent symmetry. The antenna is built on a two-sided PCB with a dielectric constant of ϵ_r 4.4.

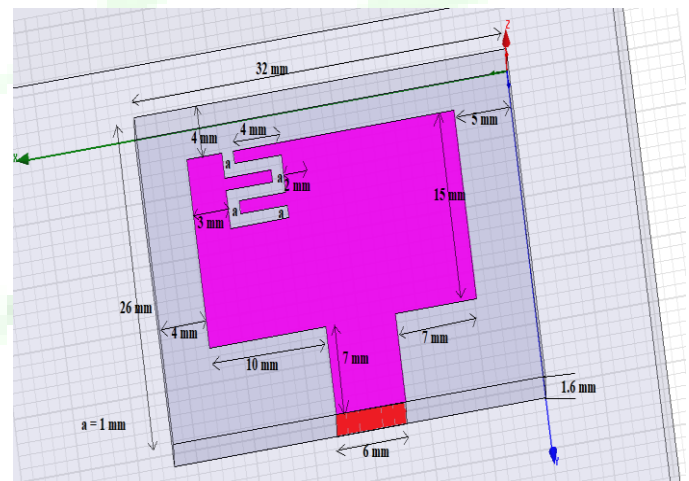


Fig. 3.1 Top view of single Meandered Slot for 1st Design Model

(b) 2nd Proposed Design with slot model

The second design is a single meandered slot impedance antenna with a microstrip feed line. The suggested antenna is 32 mm 26 mm with a 1.6 mm thickness. The feed line is 6 mm 7 mm and the excitation point is 6 mm. The 1 mm wide and 5 mm long single meandered slot impedance resonator. The patch is 23 mm 15 mm and 5 mm from the origin in x- and y-axes. This

piece contains a 1 mm 14 mm vertical slot and a meandering line, as illustrated in Figure 1.4. The highlighted area is the antenna patch. In the second design, a vertical slot is introduced near the meandered line, with 2 mm between them. Vertical slot penetration is 14 mm, and a 1 mm gap is selected from the feed line to match the meandered line gap.

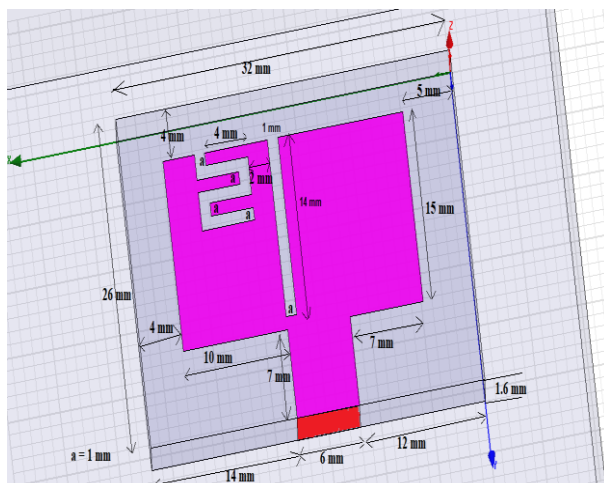


Figure 3.2 Top View of MSA for design 2

(c) 3rd Proposed Design with dual meandered slot model

The third suggested design uses twin meandered lines in two sections of patch separated by feed lines in opposing quadrants. We employ a 1 mm 14 mm vertical slot identical to design 2nd parallel to the feed line as the antenna patch. Second design adds vertical slot near meandered line; distance between slots is 2 mm. The suggested antenna is 32 mm 26 mm with a 1.6 mm thickness. The feed line is 6 mm 7 mm and the excitation point is 6 mm. Dual meandered slot impedance resonator is 1 mm wide and 5 mm long, with each meandered line 3 mm from one patch end. The patch's meandering line is coupled to a 1 mm 9 mm vertical slot (fig. 1.5). In this design, we additionally use a horizontal slit at the end of the patch with dimensions of 1 mm 8 mm. The primary patch is 23 mm 15 mm and 5 mm from the origin in x- and y-axes. Our third suggested design, a 32 mm 26 mm PCB, has the same ground plane design as the previous design. In simulation, we employed PEC, a perfect electrical conductor, instead of copper for the ground plane. Figure 4.6 shows the dimension of the proposed ground plane, which is simulated using Ansys HFSS. The antenna's substrate is a two-sided PCB made of FR-4 with a dielectric constant of ϵ_r 4.4 and a thickness of 1.6 mm.

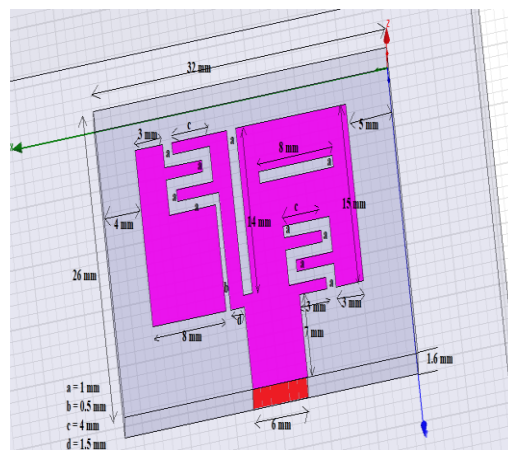


Fig. 3.3 Top View of Dual MSPA Model for design 3

(d) 4th Proposed Design with modified meandered slot model

The fourth suggested design uses twin meandered lines in two sections of patch separated by feed lines in opposing quadrants. We employ a 1 mm 14 mm vertical slot identical to design 2nd parallel to the feed line as the antenna patch. The third design adds a vertical slot towards the meandered line, with 2 mm between them. The suggested antenna is 32 mm 26 mm with a 1.6 mm thickness. The feed line is 6 mm 7 mm and the excitation point is 6 mm. Dual meandered slot impedance resonator is 1 mm wide and 5 mm long, with each meandered line 3 mm from one patch end. The patch's meandering line is coupled to a 1 mm 7 mm vertical slot (fig. 1.6). This design uses two horizontal slots at the patch's ends. Near end horizontal slot impedance is 2 mm 10 mm, far end is 2 mm 7 mm; remainder of design is same as third. The primary patch is 23 mm 15 mm and 5 mm from the origin in x- and y-axes.

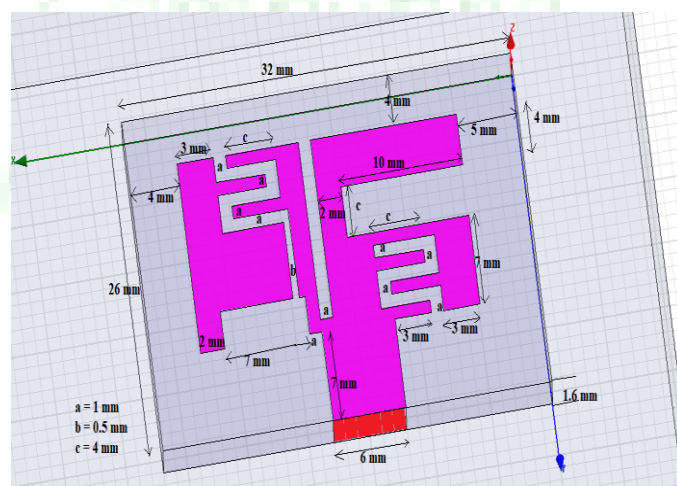


Figure 3.4 Top View of Modified Dual MSPA Model for design 4

IV. SIMULATION AND RESULTS

Result for all the Design of Single MSA based Model is listed in Table 1.1. In this part we analysis the

various performance parameter such as Peak Gain, VSWR, and Axial ratio for the all the four proposed antenna design Return loss (S11), Bandwidth, number of radiating bands

| Proposed Antenna | Radiating Frequency (GHz) | Return Loss S11 (In dB) | Bandwidth (MHz) | VSWR | Gain (dB) | Axial Ratio (dB) |
|------------------|---------------------------|-------------------------|-----------------|-------|-----------|------------------|
| Antenna 1 | 5.3 | -22.16 | 483 | 1.169 | -1.98 | 39.47 |
| Antenna 2 | 4.7 | -14.17 | 458 | 1.48 | -0.79 | 10.95 |
| | 5.7 | -25.12 | 444 | 1.11 | -0.39 | 17.76 |
| Antenna 3 | 3.6 | -15.81 | 213 | 1.38 | -2.61 | 23.98 |
| | 5.8 | -10.49 | 160 | 1.85 | 1.11 | 13.80 |
| Antenna 4 | 5.8 | -37.00 | 850 | 1.02 | 1.76 | 40.0 |

Figure 4.2 VSWR of Design 1 simulation findings

In this design, we accomplish Single-band radiation with a central frequency of 5.3 GHz, thus we'll compute performance characteristics for that frequency. First design VSWR ≤ 2 bandwidth or -10 dB return loss bandwidth is 483 MHz at 5.3 GHz centre frequency. 5.3 GHz minimum return loss is -22.16 dB. The figure 4.1, 4.2, 4.3, and 4.4 represents the above parameter like return loss S11, -1.98 dB Bandwidth gain, VSWR and Axial ratio(dB) respectively for design 1.

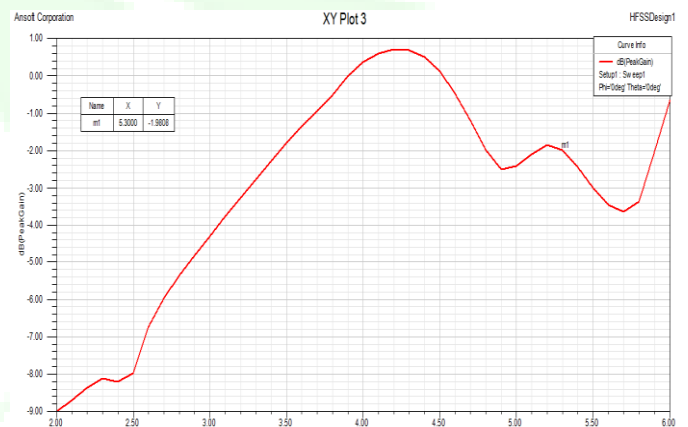


Figure 4.3 Gain in dB of Design 1 simulation findings

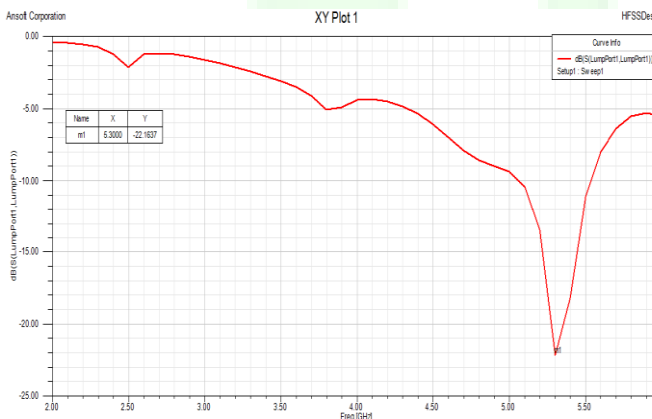


Fig. 4.1 Return loss of Design 1 simulation findings

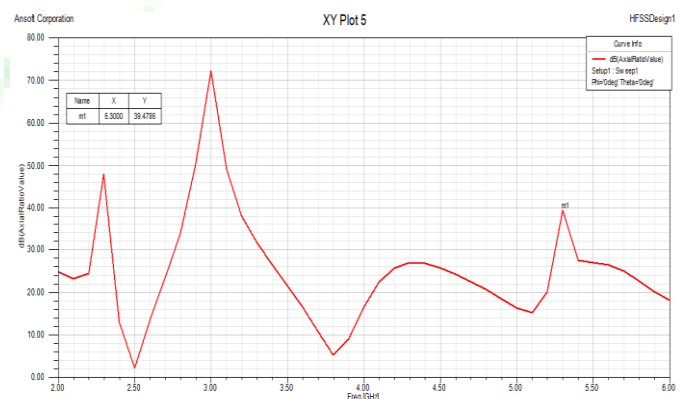
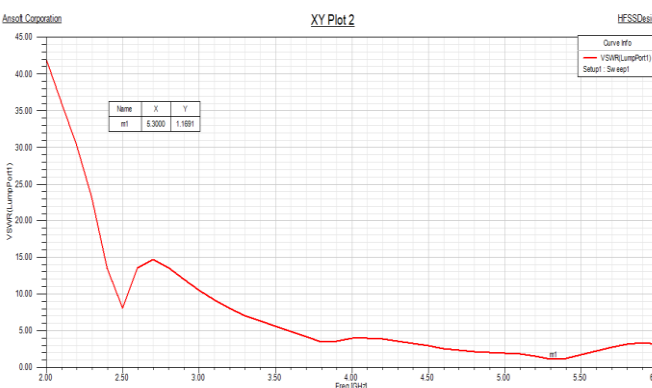


Figure 4.5 Axial Ratio in dB of Design 1 simulation findings



2nd proposal. In this design, we obtain two functioning bands at 4.7 GHz and 5.7 GHz, thus we'll compute the performance characteristics for both. In this second design, the VSWR ≤ 2 bandwidth or -10 dB return

loss bandwidth is 458 MHz at 4.7 GHz and 444 MHz at 5.7 GHz. Minimum return loss is -14.17 dB at 4.7 GHz and -25.12 dB at 5.7 GHz.

The figure 4.6, 4.7, 4.8 and 4.9 represents the above parameter like return loss S11, -1.98 dB Bandwidth gain, VSWR and Axial ratio(dB) respectively for design 2

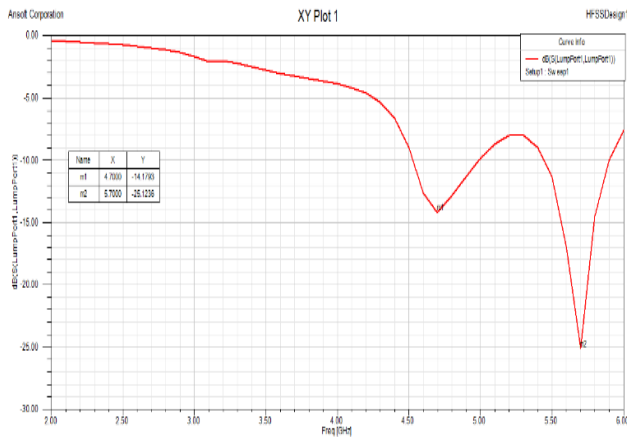


Fig. 4.6 Return loss of Design 2 simulation findings

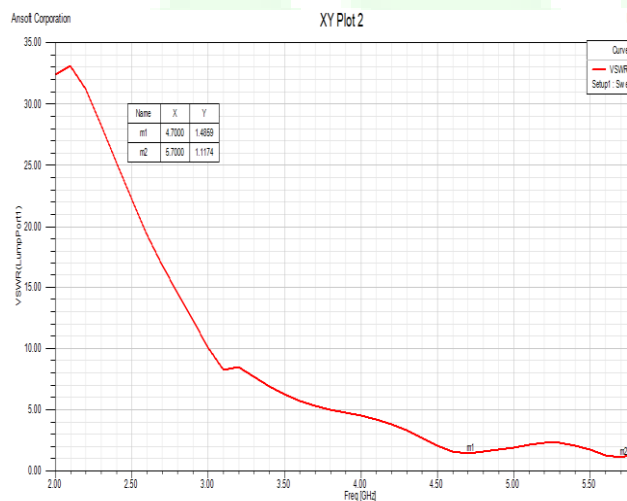


Fig.4.7 VSWR of Design 2 simulation findings

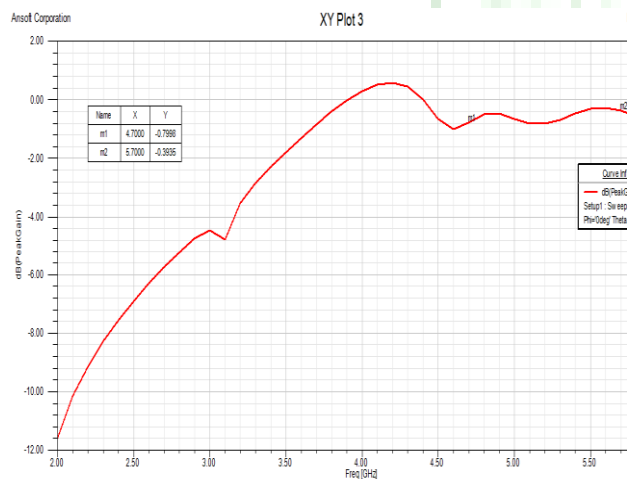


Fig. 4.8 Gain in dB of Design 2 simulation findings

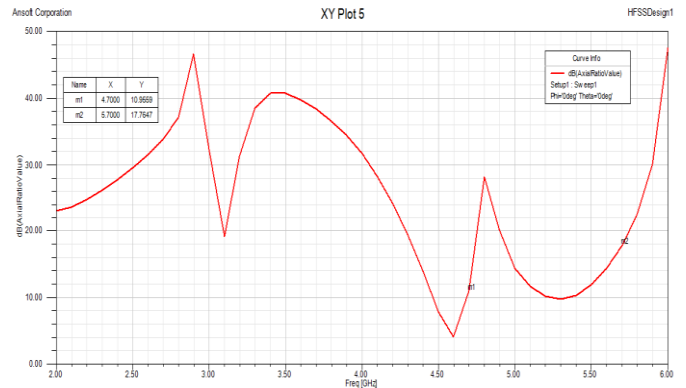


Fig. 4.9 Axial Ratio in dB of Design 2 simulation findings

3rd proposal. In this design, we accomplish dual operating bands at 3.6 GHz and 5.8 GHz, thus we'll compute distinct performance parameters for each. In our third design, the $VSWR \leq 2$ or return loss -10 dB bandwidth is 213 MHz at 3.6 GHz and 160 MHz at 5.8 GHz. Minimum return loss at 3.6 GHz is -15.81 dB, whereas 5.8 GHz is -10.49 dB.

The figure 4.10, 4.11, 4.12 and 4.13 represents the above parameter like return loss S11, -1.98 dB Bandwidth gain, VSWR and Axial ratio(dB) respectively for design 3

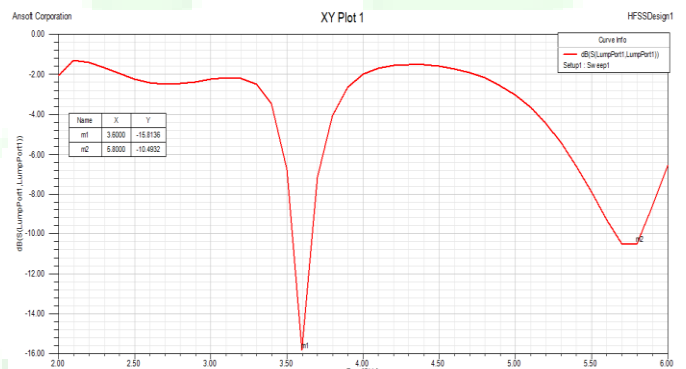


Fig. 4.10 Return loss of Design 3 simulation findings

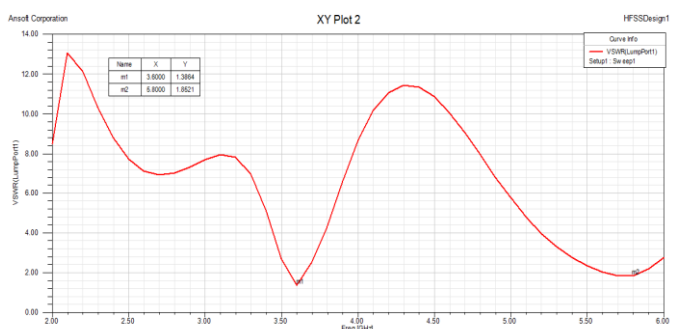


Fig. 4.11 VSWR of Design 3 simulation findings

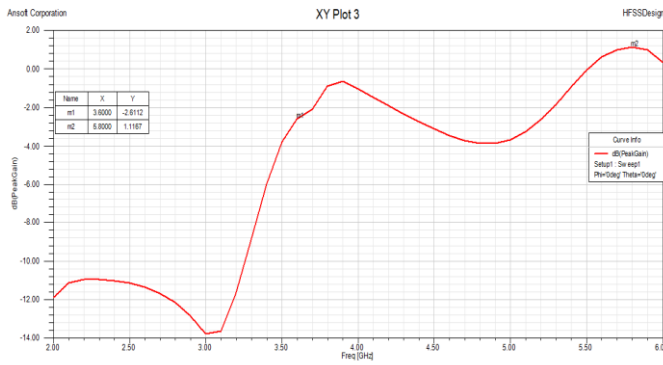


Fig. 4.12 Gain in dB of Design 3 simulation findings

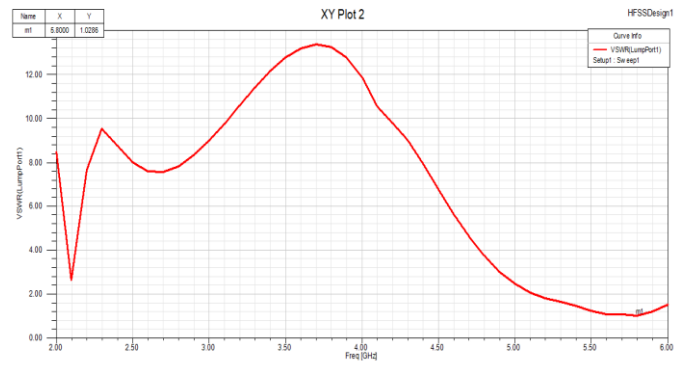


Fig. 4.15 VSWR of Design 4 simulation findings

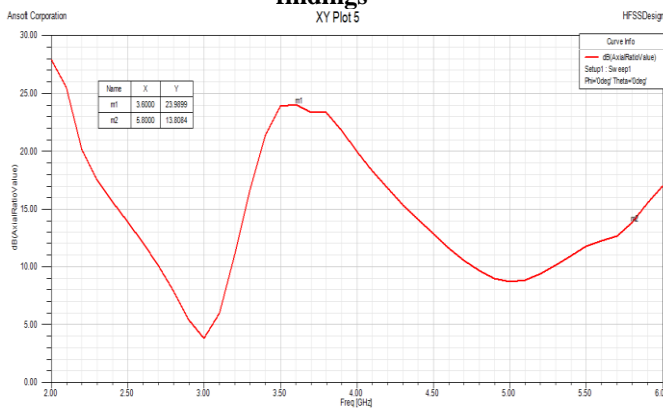


Fig. 4.13 Axial Ratio in dB of Design 3 simulation findings

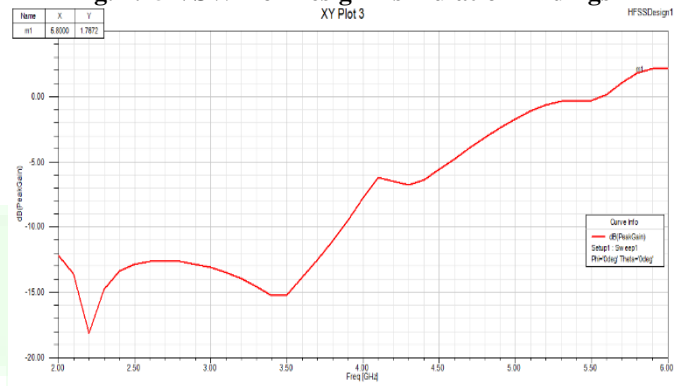


Fig.4.16 Gain in dB of Design 4 simulation findings

The fourth suggested design Because we accomplish broadband operation with a center frequency of 5.8 GHz in this design, we will compute the various performance parameters for the above frequency of operation. The bandwidth for $VSWR \leq 2$ or return loss less than -10 dB in the fourth design is roughly 850 MHz at 5.8 GHz center frequency, which is the greatest among all suggested designs. The smallest return loss at the central frequency of 5.8 GHz is -37.0 dB, which is the best among all suggested designs.

The figure 4.14, 4.15, 4.16 and 4.17 represents the above parameter like return loss S11, -1.98 dB Bandwidth gain, VSWR and Axial ratio(dB) respectively for design 4

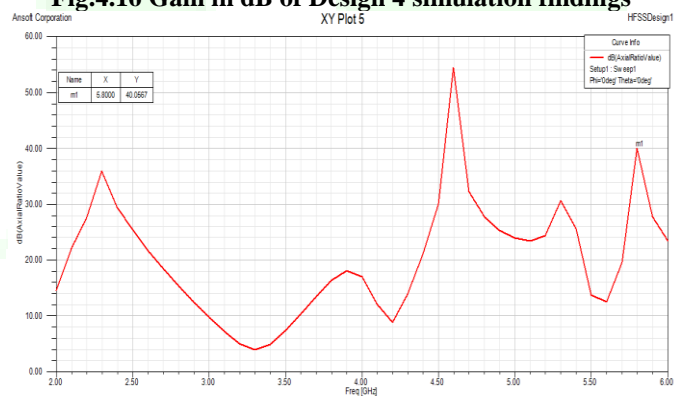


Fig.4.17 Axial Ratio in dB of Design 4 simulation findings

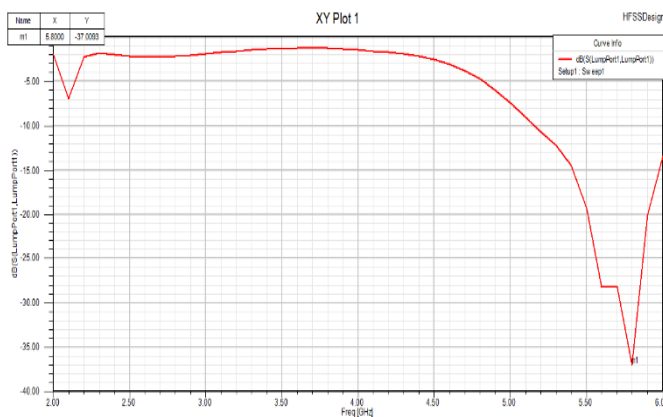


Fig. 4.14 Return loss of Design 4 simulation findings

IV. CONCLUSION AND FUTURE WORK
 This work presents a modified rectangular Patch Antenna with a meandered slot and analyses the simulation findings using HFSS. In this work, we show four patch antennas employing meandering slot patch. The first is a single meandered slot impedance structure without any additional slot lines. The third concept is a twin meandered slot impedance structure with two slots horizontally and vertically. Fourth, a modified twin meandered slot impedance structure with vertical and horizontal patch slots. Comparing all suggested designs, the 4th design has the best return loss, bandwidth, antenna gain, and VSWR at 5.8 GHz: -37.0 dB, 850 MHz, 1.02, 1.76dB. The bandwidth of the 4th design is enhanced by 431.25%, 91.45%, and 75.98% compared to the 3rd, 2nd, and 1st designs at higher simulation frequency limits (2 GHz to 6

GHz). Comparing 4th design return loss to 3rd, 2nd, and 1st design at 5.3 GHz and above, it is improved by 252.71%, 47.29%, and 66.96% as compression. Comparing antenna gain of 4th design to 3rd design at 5.8 GHz shows an increase of 58.55 percent. 4th design antenna gain is 2.15 dB bigger than 2nd design and 3.74 dB larger than 1st design.

REFERENCES

- [1] Y. Li, Z. Zhao, Z. Tang, and Y. Yin, "Differentially-fed, wideband dual-polarized filtering antenna with novel feeding structure for 5G Sub-6 GHz base station applications," *IEEE Access*, vol. 7, pp. 184718–184725, 2020.
- [2] X. Ai, Y. Liu, Y. Jia and Y. Xu, "4×4 Antenna Array for 5G Millimeter Wave Applications," *IEEE International Conference on Microwave and Millimeter Wave Technology (ICMMT)*, pp. 1-3, 2021.
- [3] Q. Hua et al., "A Novel Compact Quadruple-Band Indoor Base Station Antenna for 2G/3G/4G/5G Systems," *IEEE Access*, vol. 7, pp. 151350–151358, 2020.
- [4] C. Y. Chiu, F. Xu, S. Shen, and R. D. Murch, "Mutual coupling reduction of rotationally symmetric multiport antennas," *IEEE Trans. Antennas Propag.*, vol. 66, no. 10, pp. 5013–5021, 2018, doi: 10.1109/TAP.2018.2854301.
- [5] C. F. Ding, X. Y. Zhang, Y. Zhang, Y. M. Pan, and Q. Xue, "Compact broadband dual-polarized filtering dipole antenna with high selectivity for base-station applications," *IEEE Trans. Antennas Propag.*, vol. 66, no. 11, pp. 5747–5756, 2018, doi: 10.1109/TAP.2018.2862465.
- [6] J. Y. Jin, S. Liao, and Q. Xue, "Design of Filtering-Radiating Patch Antennas with Tunable Radiation Nulls for High Selectivity," *IEEE Trans. Antennas Propag.*, vol. 66, no. 4, pp. 2125–2130, 2018, doi: 10.1109/TAP.2018.2804661.
- [7] J. F. Li, Z. N. Chen, D. L. Wu, G. Zhang, and Y. J. Wu, "Dual-Beam Filtering Patch Antennas for Wireless Communication Application," *IEEE Trans. Antennas Propag.*, vol. 66, no. 7, pp. 3730–3734, 2018, doi: 10.1109/TAP.2018.2835519.
- [8] J. F. Qian, F. C. Chen, Q. X. Chu, Q. Xue, and M. J. Lancaster, "A novel electric and magnetic gap-coupled broadband patch antenna with improved selectivity and its application in MIMO System," *IEEE Trans. Antennas Propag.*, vol. 66, no. 10, pp. 5625–5629, 2018, doi: 10.1109/TAP.2018.2860129.
- [9] T. L. Wu, Y. M. Pan, P. F. Hu, and S. Y. Zheng, "Design of a Low Profile and Compact Omnidirectional Filtering Patch Antenna," *IEEE Access*, vol. 5, pp. 1083–1089, 2017, doi: 10.1109/ACCESS.2017.2651143.
- [10] B. Zhang and Q. Xue, "Filtering antenna with high selectivity using multiple coupling paths from source/load to resonators," *IEEE Trans. Antennas Propag.*, vol. 66, no. 8, pp. 4320–4325, 2018, doi: 10.1109/TAP.2018.2839968.
- [11] X. Chen, S. Zhang, and Q. Li, "A Review of Mutual Coupling in MIMO Systems," *IEEE Access*, vol. 6, pp. 24706–24719, 2018.
- [12] B. T. Arnold, and M. A. Jensen, "The Effect of Antenna Mutual Coupling on MIMO Radar System Performance," *IEEE Trans. Antennas Propag.*, vol. 67, no. 3, pp. 1410–1416, 2019
- [13] K. Wei, J. Y. Li, L. Wang, and R. Xu, "Microstrip antenna array mutual coupling suppression using coupled polarisation transformer," *IET Microwaves, Antennas & Propag.*, vol. 11, pp. 1836–1840, 2017.
- [14] H. Lihao, Z. Huiling, H. Zhang, and C. Quanming, "Reduction of mutual coupling between closely-packed antenna elements with split ring resonator (SRR)," in *2010 International Conference on Microwave and Millimeter Wave Technology*, 2010, pp. 1873–1875.
- [15] H. Qi, X. Yin, L. Liu et al., "Improving Isolation Between Closely Spaced Patch Antennas Using Interdigital Lines," *IEEE Antennas Wireless Propag. Lett.*, vol. 15, pp. 286–289, 2016. [16] Y. Lee, J. Yeo, and R. Mittra, "Investigation of electromagnetic bandgap (EBG) structures for antenna pattern control," in *Proceedings of the IEEE International Antennas and Propagation Symposium*, vol. 2, pp. 1115–1118, June 2003.